SciEn

Proceedings of 8th International Conference on Mechanical Engineering and Renewable Energy 2025
10-12 December, 2025, Chattogram, BANGLADESH

SciEn Conference Series: Engineering Vol. 4, 2026, pp 341-346 https://doi.org/10.38032/scse.2026.4.156

Comparative Study of Crushing Loads of Porous Aluminium- and Copper-Oxides Synthesized Via Space Holding Sintering

Mohammad Faisal, Mohammod Anwer Jahed, Md. Arafat Rahman, Shaswato Barua and Konok Chandra Bhowmik*

Department of Mechanical Engineering, Chittagong University of Engineering & Technology, Chattogram-4349, Bangladesh

ABSTRACT

Because of their many uses in energy storage, environmental remediation, catalysis, and structural materials, porous metal oxides have garnered a lot of interest. In this work, ammonium hydrogen carbonate was used as the space holder in the space holding sintering procedure to create porous copper and aluminium oxides. To create macroporous structures and promote space holder breakdown, the samples were sintered at 750 °C and pressed at 115 MPa. Aluminium oxides showed more porosity than copper oxides for the same amount of space holder content, according to optical microscopy, which confirmed non-uniform pore morphologies. Aluminium oxides produced bigger and more interconnected pores, with pore size distributions ranging from sub-millimeter to several millimetres, according to ImageJ analysis. Porosity rose as space holder content increased, reaching 66.9% for aluminium oxides and 56.7% for copper oxides at 70 weight percent. According to ASTM C365-05 crushing load testing, copper oxides have a higher crushing load than aluminium oxides while having less porosity. These findings support the strong relationship between porosity, pore shape, and mechanical strength and point to a trade-off between structural strength and porous structure in metal oxide foams.

Keywords: Metal oxides, Porous materials, Mechanical property, Hardness, Aluminum, Copper.

1. Introduction

Porous metal oxides have gained increasing attention due to a wide range of applications, including catalysis, separations, microelectronics, optics, environmental remediation, energy storage materials, and drug delivery [1-9]. In addition, it has large surface areas and pore volumes, elevated catalytic activity, and good thermal stability, which is due to the ability to interact with molecules not only at their exterior surface but also within the large interior surface of the materials [9].

Aluminum oxide (Al-oxide) foam is low density, permeable material with numerous applications. The defining characteristic of these foams is a very high porosity, typically 75-95% of the volume consisting of void spaces [2, 5]. Ceramic foam is often used for thermal insulation, acoustic insulation, adsorption of environmental pollutants, filtration of molten metal alloys, and as a substrate for catalysts requiring a large internal surface area [6]. Copper oxides (Cu-oxides) are promising materials for gas sensors, heterogeneous catalysts, photovoltaics, infrared detectors, field emission emitters and lithium-ion electrodes applications due to their unique properties such as direct band gap (1.2–1.7 eV), non-toxicity, chemical stability, abundant availability, and low production cost [7,8].

It is noted that porous foamed metals or metal oxides all suffer from deteriorating mechanical properties, such as strength, stiffness, and fatigue due to the inhomogeneous distribution and pore size [10]. However, these materials must exhibit mechanical functional property for successful applications [11]. Herein, we report the synthesis and characterization procedure of porous metal oxides, including Al- and Cu-oxides. To the best of our knowledge, this is the first report on the correlation between porosity and crushing loads of Al- and Cu-oxides.

2. Experimental Set-Up

The Cu- and Al-oxide foam fabrication process starts with the mixing of pure Cu and Al powders (Taj Scientific, Chittagong) with space holder of ammonium hydrogen carbonate (NH_4HCO_3). High purity Cu- and Al-powder (purity 99.5%) with average particle size of 5μm were used. 70 wt% of Cu- or Al-powder and 30 wt% of ammonium hydrogen carbonates were taken and ball milled at 100 rpm for 30 minutes. Similarly, 50 wt% and 70 wt% of the space holder were mixed with respective metal powders. Then, these mixtures of metal powder and space holder were subjected to green compaction. A die punch assembly was used for compaction to fabricate cylindrical samples (Height = 1.80 cm and Diameter = 1.40 cm). Compaction pressure was 115 MPa and was generated by the universal testing machine. Thereafter, the green compacted sample was sintered in an electric furnace (Nabertherm, Germany) at 750 °C for 2 h. At this temperature, the space holder (ammonium hydrogen carbonate) was decomposed and left pores in the Cu- and Al-matrix. It is noted that sintering was not carried out in an inert atmosphere; an oxide film was formed on the upper surface of the Cu- and Al-foam. The experimental setup is depicted in **Figure 1**.

Optical microscopy combined with a USB digital camera was used to characterize the morphologies (MTI, USA). Crushing load testing was performed to determine the

*Corresponding Author Email Address: arafat@cuet.ac.bd Published By: SciEn Publishing Group

mechanical properties of the samples. The applied load was at a constant rate during the testing.

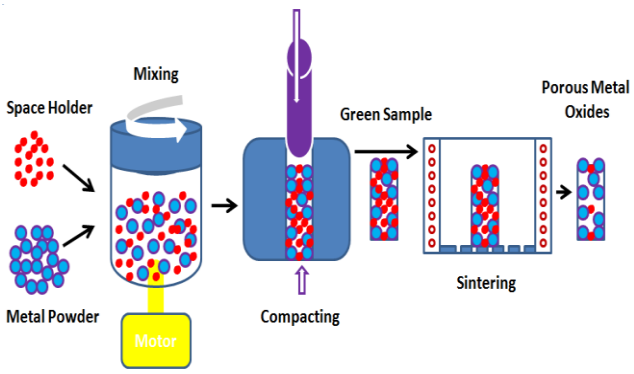

Fig. 1 Schematic diagram of experimental set-up.

3. Results and Discussion

Figure 2 depicts the plane-view optical images of porous Al- and Cu-Oxides, prepared via sintering of green samples at 750°C. The elemental analysis of the green compacted samples and those oxidized in air at 750 °C could not be conducted. However, it was reported that the formation of Cu_2O and CuO was exhibited, due to oxidation of pure Cu at 350 to 1050 °C in air [12, 13]. In addition, γ-Al_2O_3 was formed due to the oxidation of pure Al at 650 to 900 °C in air [14-16]. It is noted that the non-uniform porous Al- (**Figure 2a,c,e**) and Cu-oxides (**Figure 2b,d,f**) were clearly observed.

As shown in **Figure 2a,c,e**, the sintered Al-oxides exhibited well-developed macropores of sizes, ranging a few millimeters with patch-like regions (**Figure 2e**) due to the formation of a compact thin oxide film of aluminum. Aluminum forms a native Al_2O_3 layer in air at ambient temperature; however, the oxidation rate significantly increases at approximately 500–600 °C. Between about 700 and 800 °C, continuous and observable scale formation becomes significant, and the oxide undergoes polymorphic transitions as the temperature increases. The predominant oxidation product is γ-Al_2O_3 within the temperature range of approximately 350 to 600°C. It transitions to δ/θ-Al_2O_3 between approximately 800 and 1000 °C, ultimately reaching thermodynamically stable α-Al_2O_3 above approximately 1100 and 1200 °C. The precise temperatures at which these transformations occur are contingent upon the contaminants, particle size, and dwell duration. In addition, the compact thin oxide film is the intrinsic property of valve materials [17]. In contrast, the sintered Cu-oxides exhibited undeveloped pores in the sizes of a few millimeters and a smaller number of macropores and patch-like regions compared to Al-oxides, as shown in **Figure 2b,d,f**. It is worthy to mention that Cu reacted with space holding material and transformed to blue color even after sintering. In addition, porous Cu-oxides (**Figure 2d,f**) exhibited more cracked surface as compared to porous Al-oxides samples (**Figure 2c,e**). It is probably due to the lower stability of porous Cu-oxides at high temperature of 750 °C as compared to porous Al-oxides.

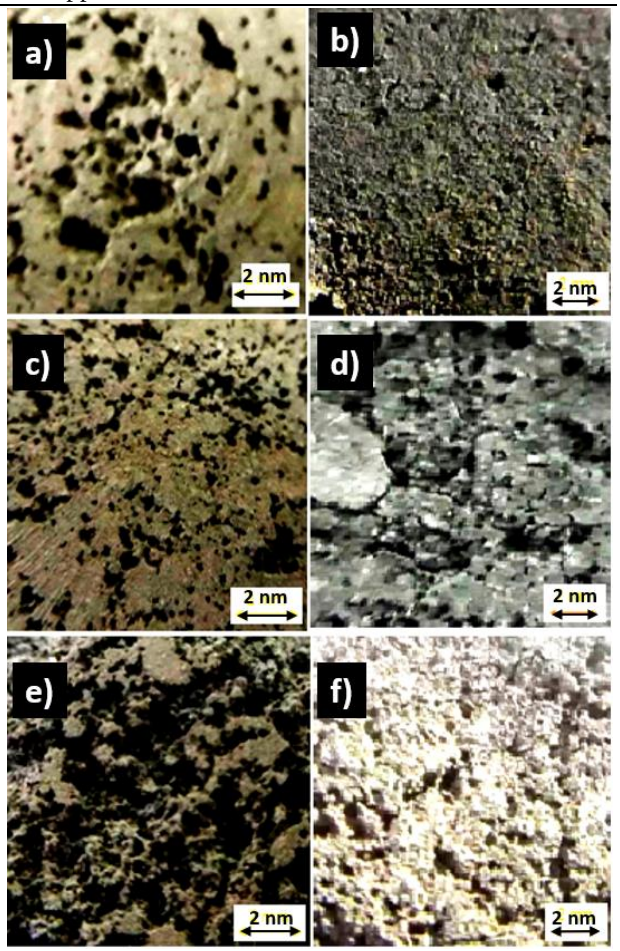

Fig. 2 Optical images of 30 wt%, 50 wt%, 70 wt% (a, c, e) Al-oxides foam and (b,d,f) Cu-oxides foam.

Figure 3 shows the frequency distribution of inner pore diameter (di) of macroporous Al- and Cu-oxides. It should be noted that the pore distribution graphs were generated from the measurements of di of optical images by using ImageJ software. The mean di of porous Al-oxides was found to be 1.20 ± 10.65 mm (**Figure 3a**), 5.25 ± 30.45 mm (**Figure 3c**), and 2.25 ± 11.50 mm (**Figure 3e**) from samples containing 30 wt%, 50 wt%, 70 wt% of space holding material after sintering in air at 750 °C. In contrast, the mean di of porous Cu-oxides was found to be 0.75 ± 3.85 mm (**Figure 3b**), 8.20 ± 60.85 mm (**Figure 3d**), and 2.45 ± 14.25 mm (**Figure 3f**) from samples containing 30 wt%, 50 wt%, 70 wt% of space holding material after sintering in air at 750 °C. It is noted that the di of porous Au-oxides ranged from 0.2 mm to 10 mm while the di of porous Cu-oxides was in a narrower range of 0.2 mm to 4.0 mm fabricated from samples contains 30 wt% space holding material. It is believed that the highly ordered pore domain of porous Cu-oxides is due to the more uniformly distributed stresses among Cu atoms due to sintering compared with Al atoms [18].

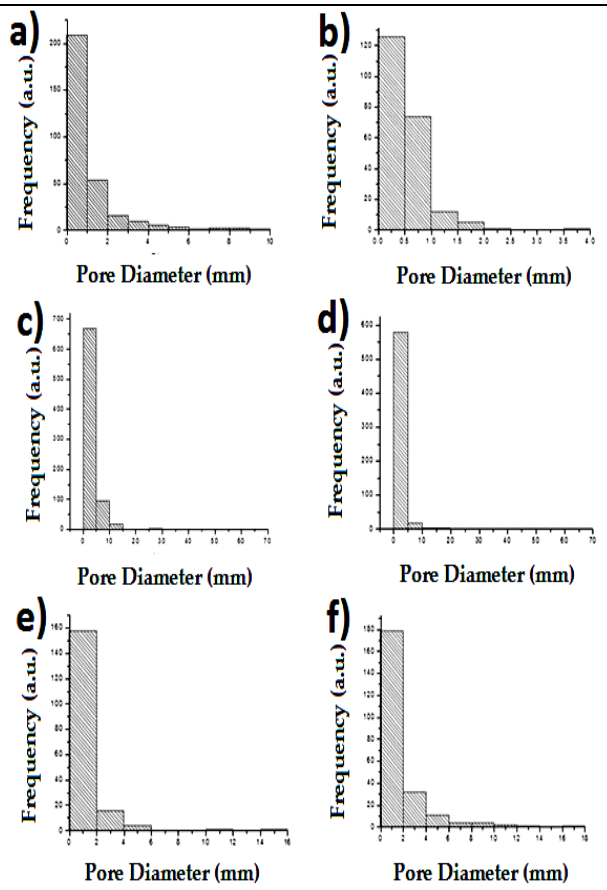

Fig. 3 Frequency distribution of optical images of samples containing 30 wt%, 50 wt%, 70 wt% space holding materials: (a, c, e) Al-oxides foam and (b,d,f) Cu-oxides foam. Note: the pore size measurements were performed by ImageJ software.

and Cu-oxides. It is probably due to the fatigue crack gradually linking between pores and following a torturous path, apparently due to localized micro/macrostructural inhomogeneities [19, 20].

Figure 4 shows the comparison of experimental porosity of as-fabricated Al- and Cu-oxides foam. It is observed that Al-oxides foam exhibited a more porous structure compared to Cu-oxides foam for samples containing 30, 50, and 70 wt% space holding material. It is probably due to the Cu reacting with space space-holding material and removing the activity of the space holder. It is noted that Cu-oxides foam fabricated through the sample contained 30, 50, and 70 wt% space holding material exhibited 7.20 ± 5.60, 17.40 ± 5.60, and 56.70 ± 2.35 % experimental porosity, respectively. However, Al-oxides foam fabricated through sample contained 30, 50, and 70 wt% space holding material exhibited 21.60 ± 2.50, 41.90 ± 3.70, and 66.90± 1.95 % experimental porosity, respectively, which is high compared with Cu-oxides foam. This phenomenon can be attributed to the lower reactivity of space space-holding material with Al-metal powder, which was observed in other similar studies [21-23].

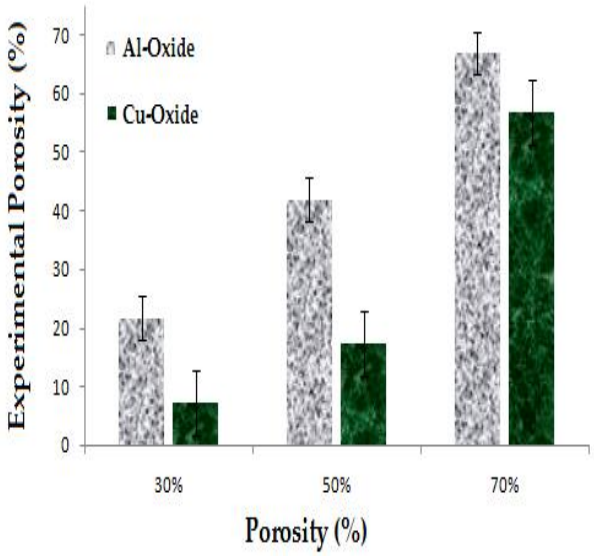

Fig. 4 Comparison of experimental porosity of porous Al- and Cu- oxides.

Uni-axial compression test was carried out in order to study the crushing load (**Figure 5**) of the Al- and Cu-oxides foam. The minimum dimension of the specimen was at least seven times the cell size to avoid size effects. In addition, all compression tests were conducted according to ASTM C365-05 standard [24].

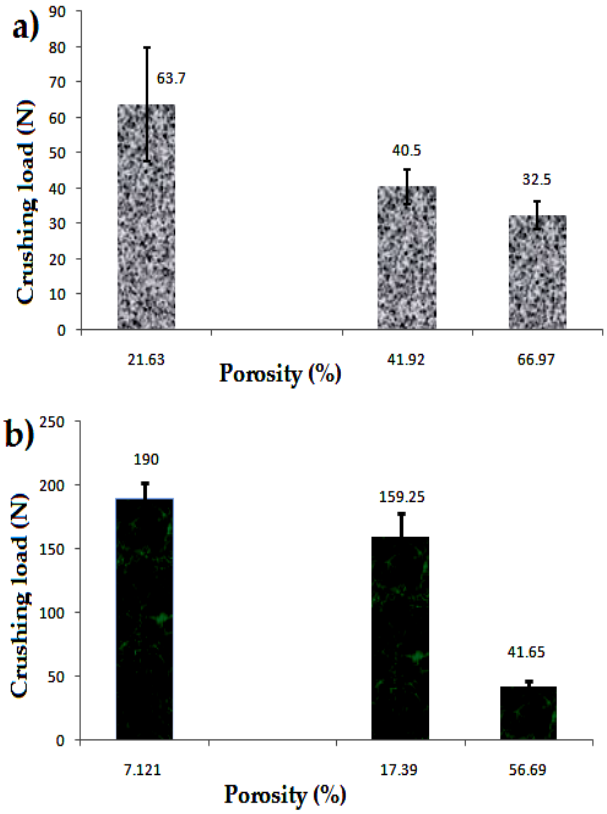

Fig. 5 Comparison of crushing load of (a) Al- and (b) Cu- oxides foam.

It was found that crushing loads of samples prepared with 30%, 50%, and 70% space holding material of Al-oxides foam are 63.70 ± 16.20 N, 40.50 ± 4.80 N, and 32.50 ± 3.95 N, respectively, which are much lower than Cu-oxides foams' crushing loads of 190.00 ± 11.70 N, 159.25 ± 18.25 N, and 41.25 ± 4.50 N, respectively. It is noted that the presence of surface defects, such as cracks and pores, both quantitatively and qualitatively changes the internal stress distributions of porous materials [25, 26]. Here, the tendency of pore formation in Al-oxides foam is very much augmented in comparison to that of the Cu-oxides, which leads to the Al-oxides foam being more vulnerable to crushing loads.

4. Conclusion

To summarize, porous Al- and Cu-oxides were successfully synthesized by space holding material, and their physical characteristics were systematically analyzed. It was observed that the pore formation tendency of Al-/Al-oxides was as high as that of Cu-/Cu-oxides with the same percentage of space holding material in green compacted samples. It is noted that the crushing load of porous Al-oxides was about 50% reduced due to the doubled pore formation, whereas Cu-oxides did not follow a similar trend. At present, the primary drawback of these materials is excessive brittleness due to ceramic properties, which leads to hindrance in the application in energy storage systems, such as electrodes of lithium-ion batteries (LIBs). The introduction of a string property with porous metal oxides could solve this problem. A significant number of studies are being carried out in pursuit of the exploration of this particular prospective segment.

5. Acknowledgement

This research is financially supported by the Nanomaterials & Energy Storage System Laboratory (NESS Lab) of Department of Mechanical Engineering and the Research and Extension Centre of Chittagong University of Engineering and Technology, Chattogram-4349, Bangladesh, through the DRE Project "Nanoporous anode materials for high-performance LIBs".

6. References

[1] Roger, C., et al., General routes to porous metal oxides via inorganic and organic templates. Journal of Sol-Gel Science and Technology, 1994. 2(1-3): p. 67-72.

[2] Banno, T., et al. Mechanical properties of micro-porous metals produced by space-holding sintering. in Advanced Materials Research. 2007. Trans Tech Publ.

[3] Tiemann, M., Porous metal oxides as gas sensors. Chemistry-A European Journal, 2007. 13(30): p. 8376-8388.

[4] Wang, C., et al., Metal oxide gas sensors: sensitivity and influencing factors. Sensors, 2010. 10(3): p. 2088-2106.

[5] Hendricks, N.R., Porous metal oxide materials through novel fabrication procedures2012: University of Massachusetts Amherst.

[6] Li, B., et al., Synthesis of hierarchically porous metal oxides and Au/TiO2 nanohybrids for photodegradation of organic dye and catalytic reduction of 4-nitrophenol. Journal of Catalysis, 2015. 329(Supplement C): p. 368-378.

[7] Hernández, P.T., S. Hailes, and I. Parkin, Hydrocarbon detection with metal oxide semiconducting gas sensors modified by overlayer or admixture of zeolites Na-A, HY and H-ZSM-5. Sensors and Actuators B: Chemical, 2017. 242: p. 1281-1295.

[8] Li, R., et al., Fabrication of porous SnO 2 nanowires gas sensors with enhanced sensitivity. Sensors and Actuators B: Chemical, 2017.

[9] Wang, Y., et al., Recent advances in ordered meso/macroporous metal oxides for heterogeneous catalysis: a review. Journal of Materials Chemistry A, 2017. 5(19): p. 8825-8846.

[10] Nakajima, H., Fabrication, properties and application of porous metals with directional pores. Progress in Materials Science, 2007. 52(7): p. 1091-1173.

[11] Seuba, J., et al., Mechanical properties and failure behavior of unidirectional porous ceramics. Scientific reports, 2016. 6: p. 24326.

[12] Bridges, D.W., et al., Oxidation of Copper to Cu2 O and CuO (600°–1000° C and 0.026–20.4 atm Oxygen). Journal of the Electrochemical Society, 1956. 103(9): p. 475-478.

[13] Mimura, K., et al., Brief review of oxidation kinetics of copper at 350 C to 1050 C. Metallurgical and Materials Transactions A, 2006. 37(4): p. 1231-1237.

[14] Jeurgens, L., et al., Growth kinetics and mechanisms of aluminum-oxide films formed by thermal oxidation of aluminum. Journal of applied physics, 2002. 92(3): p. 1649-1656.

[15] Prescott, R. and M. Graham, The formation of aluminum oxide scales on high-temperature alloys. Oxidation of metals, 1992. 38(3-4): p. 233-254.

[16] Ruano, O.A., J. Wadsworth, and O.D. Sherby, Deformation of fine-grained alumina by grain boundary sliding accommodated by slip. Acta Materialia, 2003. 51(12): p. 3617-3634.

[17] Sul, Y.T., et al., The electrochemical oxide growth behaviour on titanium in acid and alkaline electrolytes. Medical Engineering and Physics, 2001. 23(5): p. 329-346.

[18] Rahman, M.A., et al., Improvement on electrochemical performances of nanoporous titania as anode of lithium-ion batteries through annealing of pure titanium foils. Journal of Energy Chemistry, 2018. 27(1): p. 250-263.

[19] Ke, Y.-B., B. Cotterell, and Y.-W. Mai, Fracture parameters for sintered steels. Journal of materials science, 1988. 23(8): p. 2965-2970.

[20] Polasik, S., J. Williams, and N. Chawla, Fatigue crack initiation and propagation of binder-treated powder metallurgy steels. Metallurgical and Materials Transactions A, 2002. 33(1): p. 73-81.

[21] Aghion, E. and Y. Perez, Effects of porosity on corrosion resistance of Mg alloy foam produced by powder metallurgy technology. Materials Characterization, 2014. 96: p. 78-83.

[22] Zhao, X., et al., Pore structures of high-porosity NiTi alloys made from elemental powders with NaCl temporary space-holders. Materials Letters, 2009. 63(28): p. 2402-2404.

[23] Amirjan, M. and M. Bozorg, Properties and corrosion behavior of Al based nanocomposite foams produced by the sintering-dissolution process. International Journal of Minerals, Metallurgy, and Materials, 2018. 25(1): p. 94-101.

[24] Standard, A., C365, Standard test method for flatwise compressive properties of sandwich cores, 1994, ASTM C365-94. West Conshohocken, Philadelphia, Pa: ASTM International.
[25] Harris, S.J., et al., Mesopores inside electrode particles can change the Li-ion transport mechanism and diffusion-induced stress. Journal of Materials Research, 2010. 25(08): p. 1433-1440.
[26] Rahman, M.A. and C. Wen, Nanogravel structured NiO/Ni foam as electrode for high-performance lithium-ion batteries. Ionics, 2015. 21(10): p. 2709-2723.